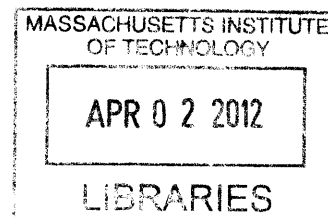# A Study of Inter-Individual Differences in the DNA Damage Response

by Meriem SEFTA,

B.S. of engineering
École Polytechnique, 2009

SUBMITTED TO THE DEPARTMENT OF BIOLOGICAL ENGINEERING IN PARTIAL FULFILLMENT OF THE REQUIREMENTS FOR THE DEGREE OF MASTER OF SCIENCE IN BIOLOGICAL ENGINEERING AT THE MASSACHUSETTS INSTITUTE OF TECHNOLOGY

DECEMBER 2011
[February 2012]
©2011 Meriem Sefta. All rights reserved.
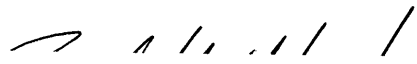
ARCHIVES

Signature of Author: _____

Meriem Sefta
Department of Biological Engineering
December 13, 2011

Certified by: _____

Leona Samson
Director, Center for Environmental Health Sciences
Professor of Biological Engineering and Biology
Thesis Supervisor

Accepted by: _____

Forest M. White
Professor of Biological Engineering
Chairman, Graduate Program Committee

A Study of Inter-Individual Differences in the DNA Damage Response

by Meriem SEFTA

Abstract

Agents that damage our DNA are omnipresent in our environment and inside our cells themselves. Left unrepaired, DNA damage can lead to premature aging, neurodegeneration and cancer. Humans have thus evolved intricate and widespread mechanisms to repair and manage this damage. These mechanisms—called the DNA damage response—often involve cell cycle arrest. Cell cycle arrest gives the cells precious extra time to utilize its diverse set of repair pathways. Among these is the homologous recombination pathway, which repairs DNA double-strand breaks. When the damage is deemed irreparable, a cell can choose to die: this allows for the maintenance of genomic integrity of the organism.

Humans share 99.9% of the same genetic information. The remaining 0.1% is responsible for all genetic variations between individuals. This includes differences in disease susceptibility. In this study, we examined the inter-individual differences in the DNA damage response. To do so, we used a panel of twenty-four B lymphoblastoid cell lines derived from twenty-four healthy individuals of diverse ancestries. This panel had already been shown to display a broad range of sensitivity to several DNA damaging agents.

We focused our attention on the alkylating agents temozolomide and methylnitronitrosoguanidine (MNNG). While MNNG has been extensively studied as a model DNA damaging drug, temozolomide is used in the clinic today to treat astrocytoma and glioblastomas. The two drugs are often referred to as functional analogues. We wanted to see if the cell lines' relative sensitivities to both drugs would be similar, which would support the analogy made between the drugs, or different, which would refute it. Furthermore, we measured the amounts of sister chromatid exchanges (SCEs) induced by temozolomide treatment to determine if the sensitivity measured by growth inhibition post-treatment was correlated with the amount of temozolomide-induced SCEs. For the cell lines tested, we found that the MNNG-induced sensitivity was similar to that induced by temozolomide. We also found a cell line in which temozolomide induced a large growth inhibition, all the while inducing no detectable SCEs.

Thesis Advisor: Leona Samson
Title: Professor of Biological Engineering and Biology, Director, Center for Environmental Health Sciences

Acknowledgments

First and foremost, I would like to thank my advisor, Professor Leona Samson, for her support and guidance over the past years. I am very grateful to have been given such an exciting project to work on.

Besides providing excellent opportunities for research, the Biological Engineering department has provided me with excellent classes and great professors. These professors have mentored me throughout my Master of Science degree, and I am particularly grateful for the help and support of Douglas Lauffenburger, our department head.

I would like to thank past and present members of the Samson lab. Whether it be by teaching me new experimental techniques, by helping me with my project design, or just by being supportive friends, they have tremendously helped me with this project, and made the Samson lab a truly collaborative and fun place to work.

I would like to acknowledge the Koch Institute flow cytometry facility where all the flow cytometry data were obtained. I would especially like to thank Glenn Paradis for training me and helping me troubleshoot my flow cytometry experiments.

Last but definitely not least, I would like to thank my friends and family. My friends at MIT—and particularly the ones in the Biological Engineering department—have made MIT a fun place to work, and continue to give our department a fun and unique flavor. My parents and sister have been unconditionally supportive during these past two years, and I would be lost in the world without their emotional support, great practical advice, and overall dedication.

Table of Contents:

Figures and Tables

Introduction

1. DNA damage and the DNA damage response

DNA damaging agents are omnipresent, whether it be in our environment, or inside our bodies themselves. The exogenous sources of DNA damage include UV radiation from sunlight, elements in our food and drinks, and chemical pollutants. Some chemotherapeutic agents used in the clinic today to treat cancers also function as DNA damaging agents. The endogenous sources of DNA damage are just as varied. Our cells' metabolism, as well as their inflammatory responses generate reactive oxygen species and reactive nitrogen species that can cause DNA lesions [7][8]. Furthermore, our cells also have to manage DNA's intrinsic chemical instability, as well as its replication errors [9]. In total, it is estimated that each of our cells is faced with 10^5 DNA lesions each day. [6]

Unrepaired DNA damage can have harmful consequences. At the cellular level, it can lead to mutations, chromosomal aberrations, cell cycle delay or arrest, and cell death [10]. These effects have consequences at the organism level; they can lead to cancer, premature aging, neurodegeneration, tissue toxicity and endothelial damage [11][6].

In order to counteract DNA lesions, humans have evolved a very broad and intricate response system—called the DNA damage response (DDR)—that is triggered in our cells in the presence of damage. This response is initiated when sensors detect damage; the signal is amplified through the recruitment of mediators and then of transducers and effectors that lead to diverse cellular responses [12].

When a cell deems that the damage is too great, it can trigger its own cellular death. If it does not die, a cell can arrest itself, thus providing crucial extra time for the repair machineries to process the damage. If residual damage is left at the time

of DNA replication, mutations and chromosomal aberrations can arise. This can eventually lead to cancer [13,14] (figure 1).

The types of damage that can occur in our DNA are diverse. As a consequence, the DNA repair processes that our cells have evolved are also diverse. Small DNA adducts can be removed through direct reversal by proteins like O^6-methylguanine-DNA methyltransferase [15] [16]. Base excision repair (BER) is also solicited in the case of small, non-helix-distorting base lesions in the genome. In BER, a DNA glycosylase recognizes the lesion, flips the damaged base out of the double helix, and cleaves the N-glycosidic bond of the damaged base, leaving an abasic site. DNA is then nicked at this site, and several enzymes are recruited to fill and ligate the resulting DNA [17]. In the case of helix-distorting lesions or pyrimidine dimers like the ones induced by UV damage, nucleotide excision repair (NER) often comes into play. The enzymes involved in NER will successively recognize the lesion, locally unwind the DNA, remove a single stranded stretch of 25-30 nucleotides, then fill and ligate the gap [18]. Homologous recombination is the process by which cells repair double-strand breaks by using a homologous template[19], while in non-homologous end-joining, the break ends are directly ligated without the need for a homologous template[20]. Finally, a cell can call upon translesion synthesis, a DNA damage tolerance process that allows the DNA replication machinery to replicate past DNA lesions [21].

The effects and importance of all the varied signals initiated after DNA damage are still not completely understood and are active areas of research. Several genome-wide screens for genes conferring susceptibility for DNA damage have revealed that the DNA damage response actually involves a great multitude of actors and processes in the cell. These actors haven't all been fully characterized [22] [23].
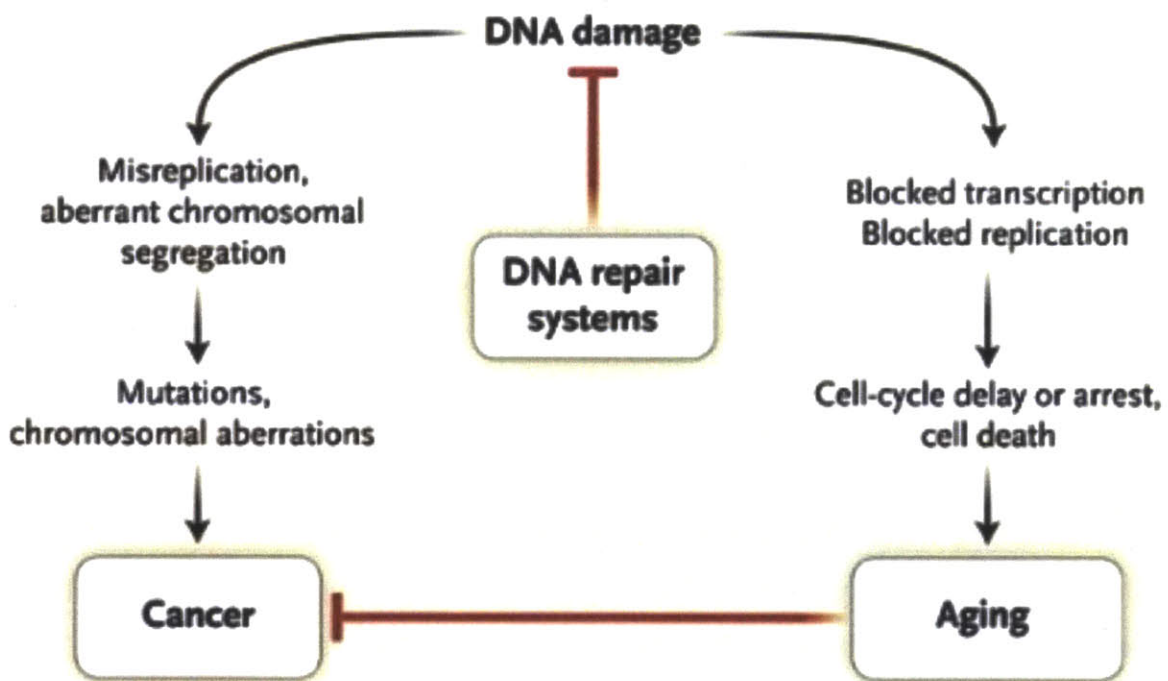
Figure 3: The effects of DNA damage on a cell

Adapted from [6]

2. The Cell decision process

In a multicellular organism, the process by which some cells chose to die in the presence of damage that is deemed irreparable is crucial for the maintenance of that organism's genomic integrity. A cell that decides against death despite the presence of damage can accumulate mutations or chromosomal aberrations, two hallmarks of cancer [24]. If the cells of an organism chose to die too frequently, it is also detrimental, as it can lead to unwanted cell death and premature tissue aging[25]. Many elements are known to factor into this decision, and experimental evidence shows that it depends on the cell type and on the amount of damage.

The cell decision process is frequently deregulated in cancer. The p53 tumor suppressor gene, called the "guardian of the genome", has been shown to be a master player in this process. p53 is mutated in 50% of all cancers [26].

3. Of inter-individual differences and personalized therapies

Humans share 99.9% of the same genetic information. The genetic diversity of the human race as we know it is contained in the remaining 0.1%. Learning about the genetic difference between humans can be used to understand population history, trace lineages, analyze natural selection trends, and—above all—to predict disease susceptibility[27].

The genetic variations in human populations are varied. A Single Nucleotide Polymorphism (SNP) refers to a DNA sequence variation of a single nucleotide within a sequence that is present in 1% or more of the population; over ten million such variants have been identified and validated in the human population. A short tandem repeat (STR) in DNA occurs when a pattern of two or more nucleotides is repeated and the repeated sequences are directly adjacent to each other. In human populations, a short tandem repeat polymorphism (STRP) occurs when homologous

STR loci differ in the number of repeats. There are currently over 10 000 published STR sequences in the human genome. Finally, insertions or deletions of certain parts of the DNA sequence in different individuals also contribute to human genetic diversity[28].

These genetic variations can have consequences at the level of the cell, and of the whole organism. It is therefore not surprising that several of them have been implicated in disease susceptibility, and in patient response to a number of therapeutic drugs. Today however, only about 10% of labels for FDA-approved drugs contain pharmacogenetic information[29]. In the case of cancer drugs, most of these drugs are only efficient in a small fraction of patients. Patients generally have to change drug treatment strategies several times before an efficient one is found, if ever. In order to improve the success rate of these drugs, it is becoming clear that treatment strategies must become more personalized [30,31]. Beyond personalized treatment, health care today is also aiming towards becoming increasingly capable of predicting and preventing cellular dysfunction and disease[32,33].

The DNA damage response is no exception to these inter-individual variations. It has been shown that human populations display a broad range of sensitivities to different DNA damaging agents [3] (figure 2).

Numerous single genetic variants have been directly linked to disease states. For instance, this is the case for sickle-cell anemia, where a single base mutation is responsible for the disease[34]. However, an increasing body of work is revealing that each inter-individual polymorphism usually only leads to very subtle variations in the cell, if any. A systems-wide approach is therefore necessary to integrate all of the variations between individuals, and infer their influence—as a whole—on cellular and organism processes[35].
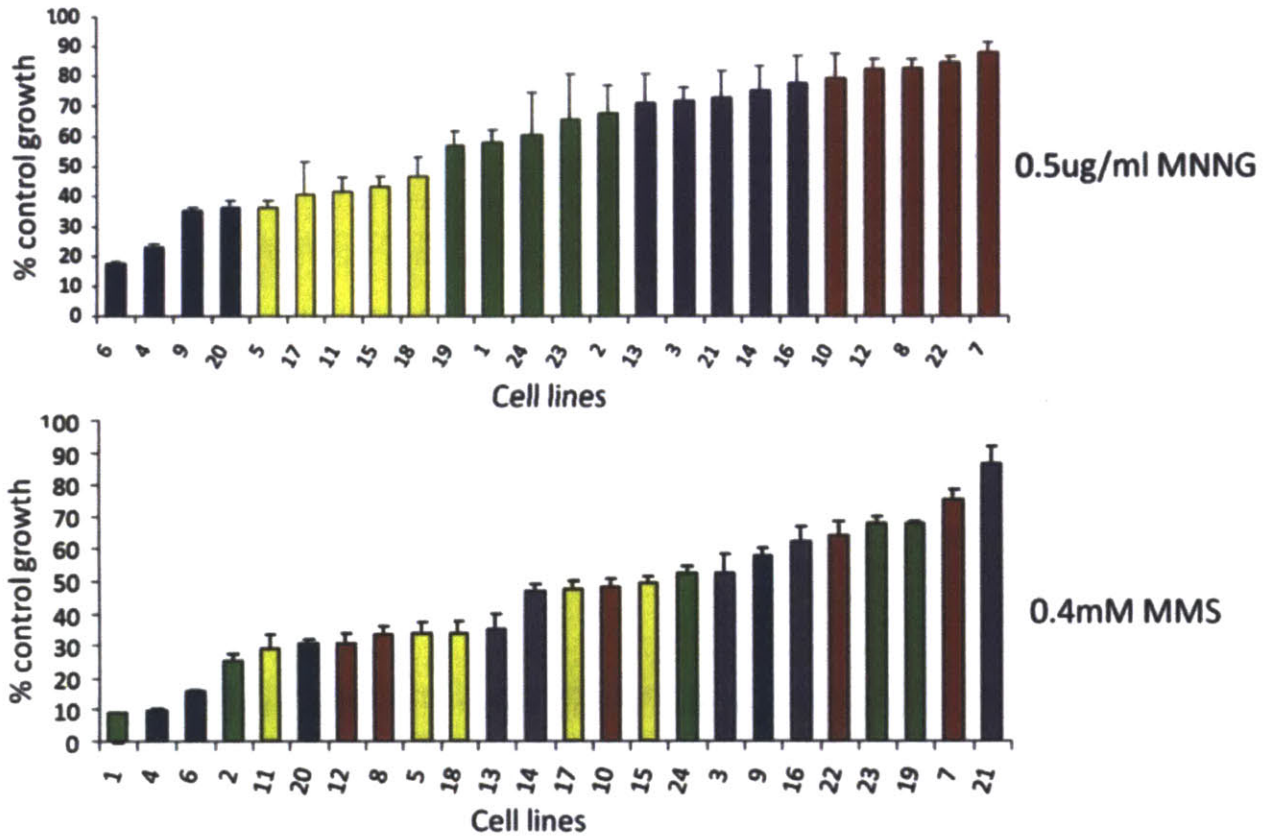
Figure 4: A panel of 24 cell lines derived from 24 healthy individuals of diverse ancestry shows a broad range of sensitivity to MNNG and MMS

MNNG sensitivity (top) [3] and MMS sensitivity (unpublished data, Samson Lab) of the panel of cell lines. Cell lines are colored according to MNNG sensitivity to show the different order of sensitivity for MMS (figure from Leona Samson)

4. Experimental system used to study the DDR in different individuals

Temozolomide, MNNG, and the DNA damage response they initiate:

Temozolomide is a chemotherapeutic drug used in the clinic today. It can be used for the treatment of Grade IV astrocytoma — an aggressive brain tumor, also known as glioblastoma multiforme, as well as anaplastic astrocytoma. It has been available in the US since August 1999, and in other countries since the early 2000s[36] [4].

At physiologic pH, temozolomide is converted to the short-lived active compound MTIC (*3-methyl-(triazen-1-yl)imidazole-4-carboxamide*). While MTIC can react with cellular proteins, the cytotoxicity of MTIC is due primarily to the O^6-methylguanine (O^6MeG)and 3-methyladenine (3MeA) methylation adducts [37] (figure 3).

In the presence of temozolomide, cells activate their DNA damage response. The first step in the repair process most notably involves the use of the O^6-methylguanine-DNA methyltransferase (MGMT) repair protein. MGMT is a direct reversal suicide enzyme that directly removes methyl adducts from O^6MeG DNA bases [38] (figure 5). If replication occurs before a given O^6MeG lesion has been repaired, the replication machinery will mistake the guanine for an adenine and pair it with a thymine, thus creating a mismatch. An accumulation of mismatches can directly signal for cell death. If the cell decides to survive, and the mismatch repair machinery does not process this error, the mismatch will lead to a permanent mutation at the next round of replication. When the mismatch repair machinery does attempt to repair the mismatch, it is believed that since the cell will remove the newly synthesized one, ie the thymine; the mismatch repair machinery will again pair a thymine with the O^6MeG; this leads to a futile repair cycle where the damaged

base never gets removed[39]. This cycling eventually leads to replication fork collapse and double strand breaks. Finally, double strand breaks can also signal for cell death, or be processed through homologous recombination [40,41]. (figure 6)

Methylnitronitrosoguanidine (MNNG) is a biochemical tool used experimentally as a carcinogen and mutagen [42] (figure 4). Its cytotoxicity is also primarily due to the O^6MeG and 3MeA adducts, and MGMT is also strongly solicited in response to MNNG induced damage. As a consequence, MNNG is often used as a functional analogue of temozolomide [40,43-45]. While the main cytotoxic lesions of MNNG are the same as those of temozolomide, the other effects that both drugs have on a cell could very well be different, and make the overall sensitivity of a given cell line to each drug different.

For these reasons, we decided to investigate the DNA damage response to temozolomide and to MNNG in different individuals.
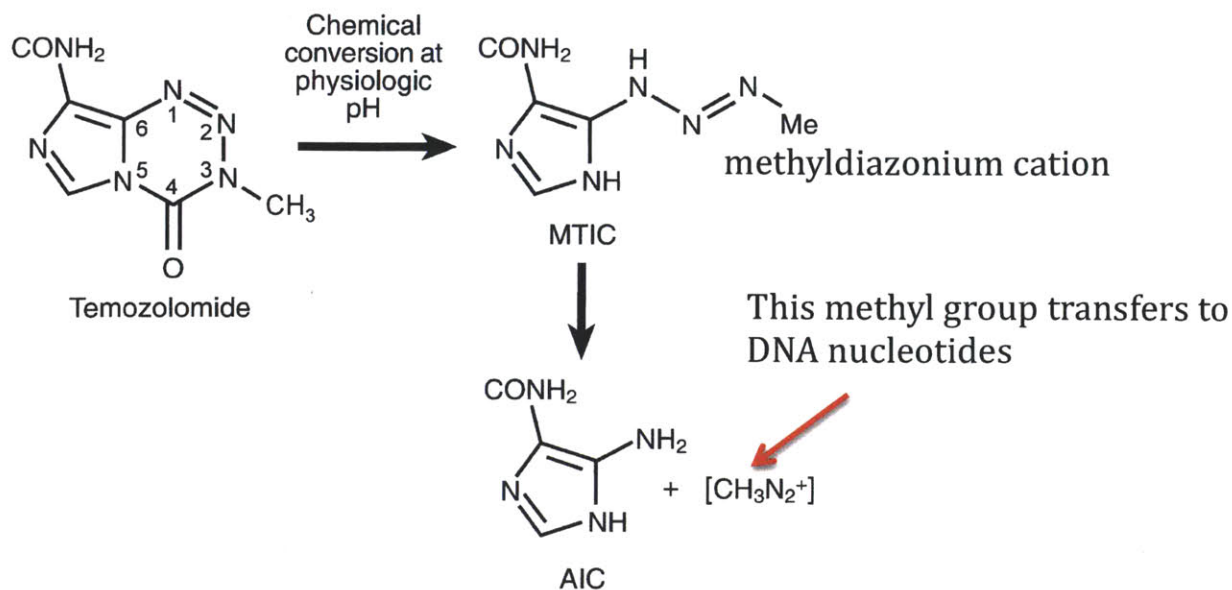
Figure 3: Temozolomide undergoes spontaneous conversion under physiological conditions to the active alkylating agent MTIC.

Its main cytotoxic lesions are methylation of N^7 position of guanine, and methylation at the O^6 position of guanine (5%) (adapted from [4])

N-Methyl-*N'*-nitro-*N*-nitrosoguanidine
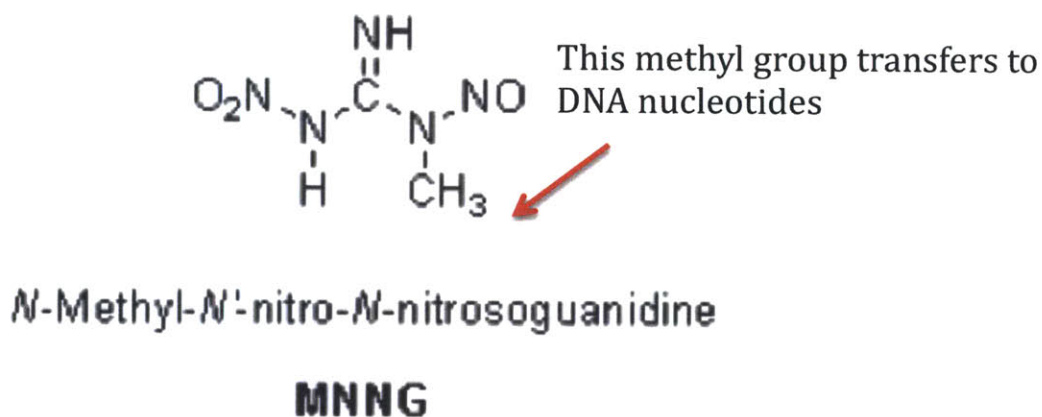
MNNG

Figure 4: Chemical structure of MNNG

Its main cytotoxic lesions are 3MeA and O^6MeG (5%)

adapted from the Sigma-Aldrich website page
http://www.sigmaaldrich.com/chemistry/chemical-synthesis/technology-spotlights/diazald.html)
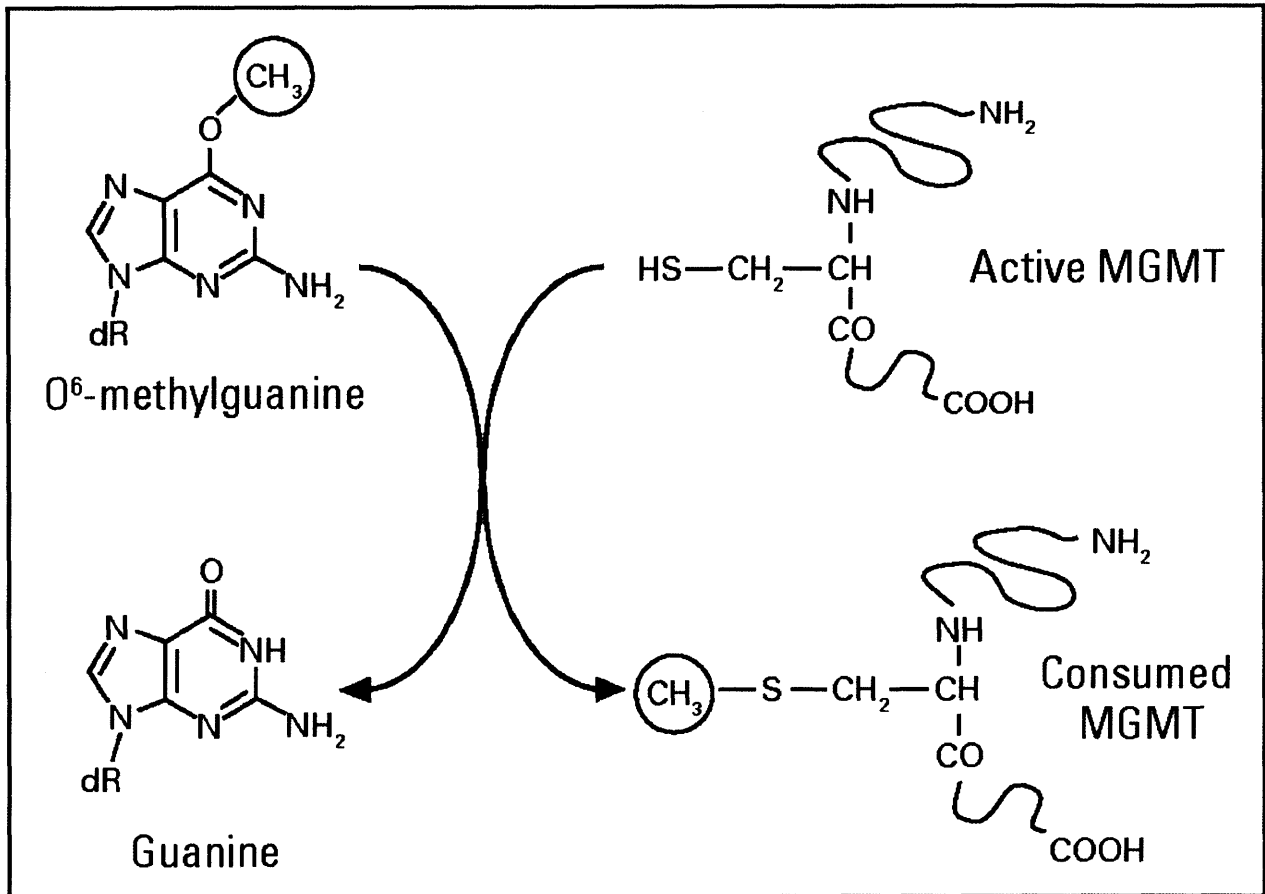
Figure 5: MGMT is a direct reversal suicide enzyme that can remove methyl adducts created by temozolomide or MNNG

adapted from [2]
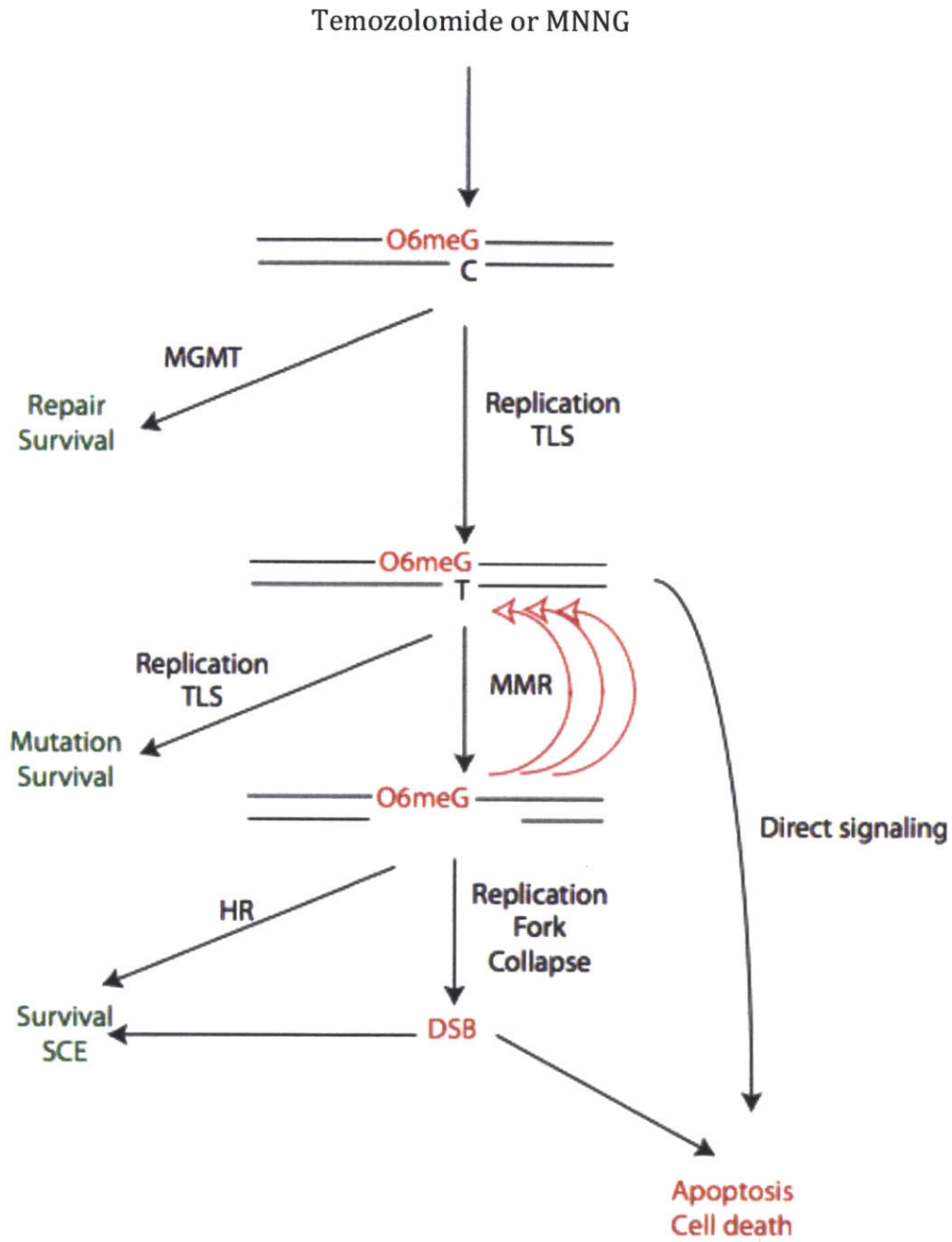
Figure 6: Models of mismatch repair dependent cytotoxicity

Adapted from a figure by D. Fu, J. Calvo and L. Samson (Nature Reviews Cancer, 2012, *in press*)

SCE: sister chromatid exchanges, induced by homologous recombination
TLS: translesion synthesis
DSB: double strand breaks

The Coriell panel of cell lines:

We focused our attention on a panel of twenty-four genetically diverse cell lines. These twenty-four cell lines are a subset of a larger set of 450 B lymphoblastoid cell lines; the subset maintains the diversity of the larger set [46]. All of them were derived from the blood of healthy United States citizens with ancestries from around the globe. B lymphocytes were purified from the blood samples, and then immortalized by Epstein Barr Virus (EBV) transformation. Since EBV transformation does not affect p53 function, it is a reasonable assumption that the DNA damage response in these cell lines is a mirror of what it is in the different individuals. [47]

Previous work conducted by Samson and colleagues has shown that these cell lines display a broad range of sensitivity to the DNA alkylating agents MNNG (figure 2). Using computational machine learning techniques, they successfully identified 48 genes with basal expression that predicts susceptibility with 94% accuracy. This leads us to believe that the panel of twenty-four cell lines is a good experimental system to pursue studies on inter-individual differences in the DNA damage response [3].

5. Goal of the study and project design

The goal of this thesis was to i) measure the sensitivity of the panel of twenty four cell lines to the cytotoxic agents temozolomide and MNNG using a high-throughput growth inhibition assay developed in the Samson lab[5]; ii) in the case of temozolomide, also measure the drug's induction of SCEs—a surrogate marker for homologous recombination events, in order to compare this data to the growth inhibition data.

Results and Discussion

1. A high-throughput growth inhibition assay is used to measure temozolomide and MNNG induced cytotoxicity and cell cycle effect.

Introduction:

Temozolomide and MNNG are two alkylating agents that are often used interchangeably in the scientific community as they are thought to be analogues. Their main cytotoxic lesions are 3MeA at the O^6MeG (figures 3 and 4). However, they also react with the proteins of a cell, and these reactions could be different for both drugs. Furthermore, these drugs could have differing cytotoxicity kinetics. As a consequence, a given individual may have differing sensitivities to both drugs.

To investigate this possibility, we worked with a panel of twenty-four cell lines derived from twenty-four United States individuals. Previous work on these cell lines from the Samson lab has revealed that they display a very broad range of sensitivity to MNNG. It has also been shown that a cell line that is very resistant to one source of damage can be sensitive to another. We wanted to determine i) if the 24 cell lines display as broad of a range of sensitivity to temozolomide as they do to MNNG and ii) if the order of the cell lines in this range is the same for both drugs.

We used a high-throughput growth inhibition assay for measuring the sensitivity of the cells. This assay was developed in the Samson lab, and has a dynamic range comparable to that of the slower clonogenic survival assay, the current gold standard for assessing cellular growth inhibition after DNA damage[5]. In the high-throughput method, BrdU—a thymidine analog—is added to the media of cells. As the cells proliferate, they incorporate the BrdU into the A-T rich regions of

their DNA. Hoechst, a dye that preferentially binds AT-rich regions in the DNA, is quenched by BrdU. Cells that have divided zero, one or two times in the presence of BrdU can therefore be differentiated based on the level of quenched Hoechst fluorescence, thus giving a measure of cell proliferation.

After cells were treated with temozolomide or MNNG, they were allowed to recover for the duration of two doubling times, and then left to proliferate in the presence of BrdU for another two doubling times (as shown in figure 7). The cells were subsequently lysed to extract their nuclei and stained with Hoechst dye and propidium iodide (PI). Figure 8 illustrates how this experimental set up allowed us to distinguish first cell cycle nuclei from second and third cell cycle nuclei, as well as G1 phase nuclei from S/G2 phase nuclei. The PI and Hoescht fluorescence of the nuclei were measured by flow cytometry. Figure 9 shows the kinds of plots we obtained, and how the data was gated and analyzed. The relative growth inhibitions of treated samples versus mock treated samples give reproducible measures of the sensitivity of the cells to treatment.
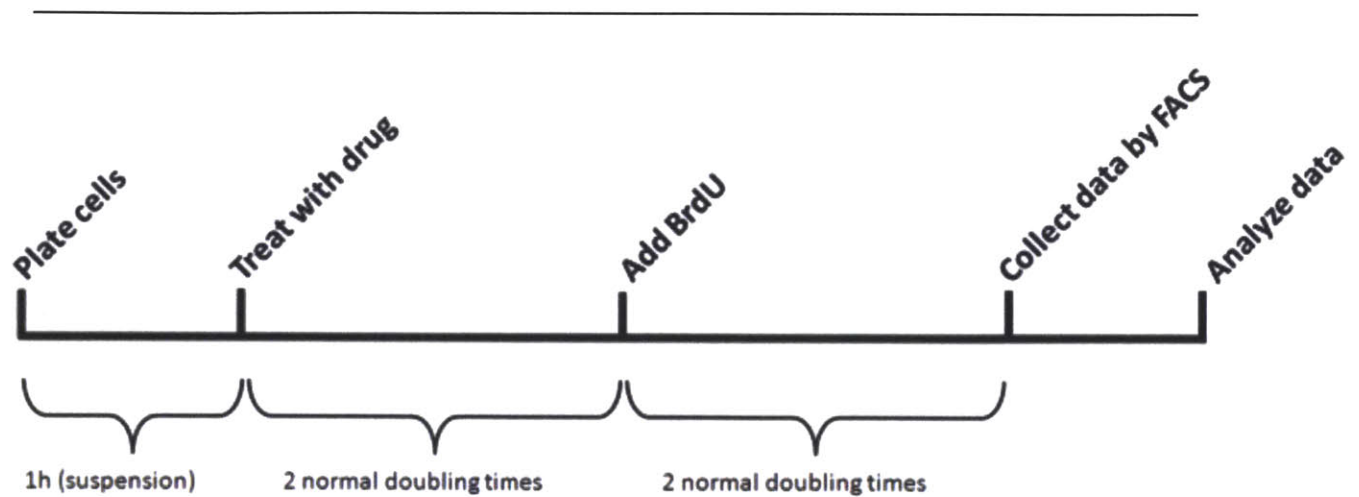
Figure 7: Experimental setup for the high-throughput growth inhibition assay used to measure sensitivity or the Coriell panel of cell lines to MNNG and temozolomide

- Hoechst is a fluorescent dye that binds to AT rich regions of DNA. Fluoresces less efficiently when bound to poly (dA-dBrdU) than when bound to poly (dA-dT).

- PI measures the total amount of DNA in a given cell, so it is indicative of the PHASE of the cell cycle.
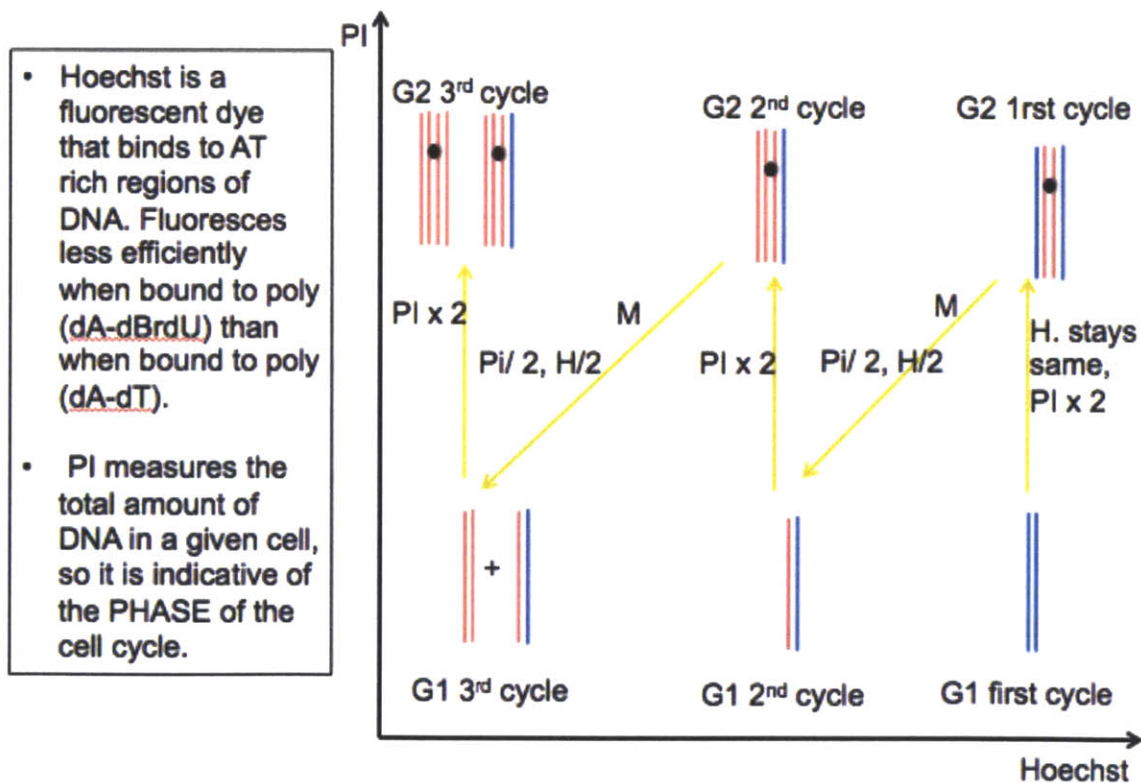
Figure 8: Schematic representation of what how Hoechst and PI allow us to determine what cell cycle the nuclei are in, and in what phase

DNA strands that have incorporated BrdU are represented in pink, those that have not are represented in blue.
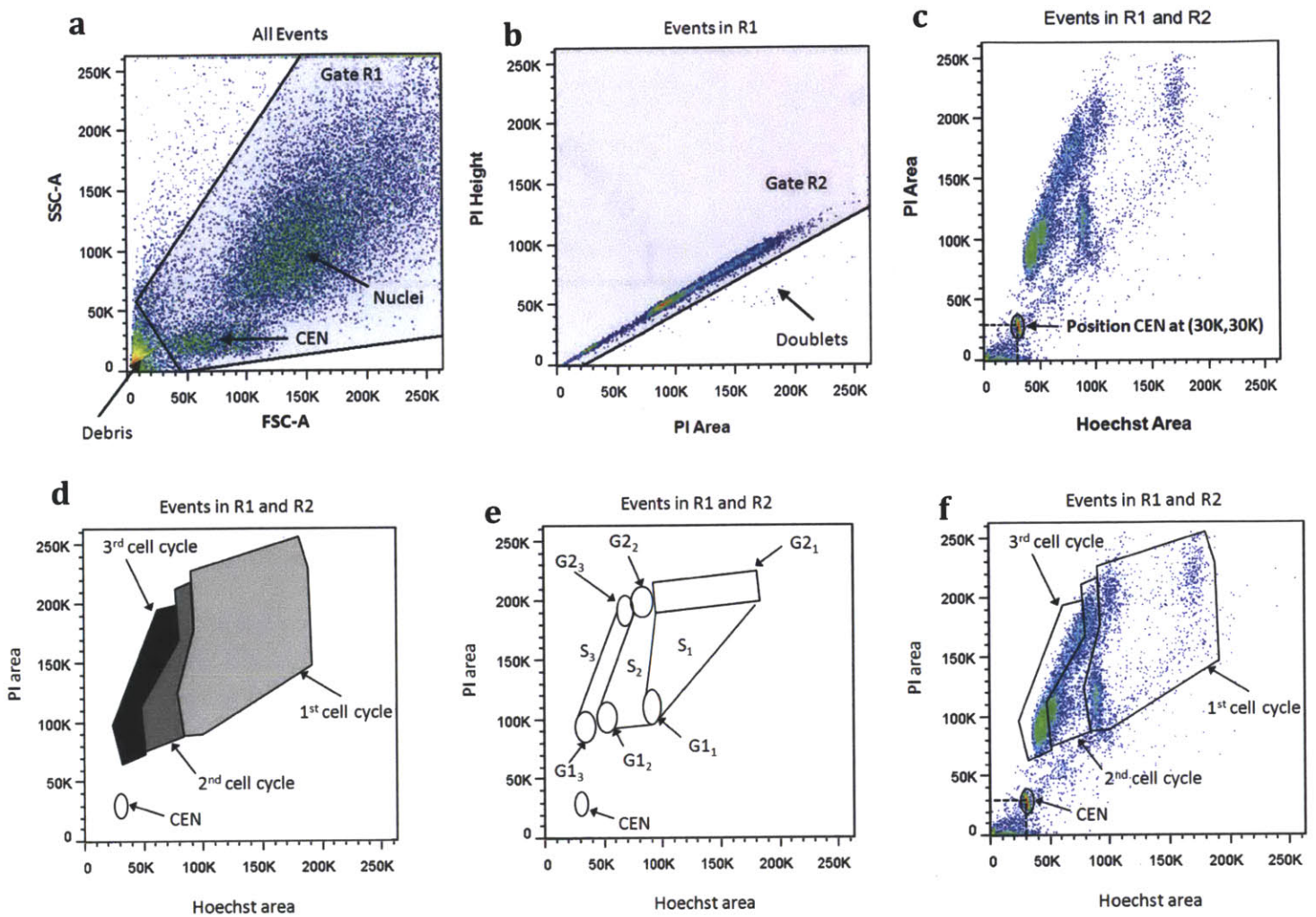
Figure 9: Flow cytometry data analysis methodology (adapted from [5])

Panels a, b and c show how we filtered the raw data:
a) Side scatter vs. forward scatter plot shows the position of nuclei, chicken erythrocyte nuclei (CEN) and the debris. We start by excluding the debris by creating gate R1
b) These are the events in gate R1. In this PI-Height vs. PI-Area plot, the events that fall below the drawn diagonal must be excluded, as the correspond to cell doublets that cannot be taken into account in our analysis.
c) These are the events in gate R2; PI-Area vs. Hoechst-Area of these events is plotted. During data acquisition, PI and Hoechst channel voltages were adjusted to position the CEN at (30K, 30K)

Panels d, e and f show how we gated the filtered data (PI-Area vs. Hoechst-Area plots):
d) The light grey area is where the nuclei in the first cell cycle would fall, the dark grey is where the ones in their second cell cycle would fall, and finally the one in black is where the third cell cycle nuclei would fall.
e) This plot shows the G1, S and G2 populations for each cell cycle.
f) Example of a sample for which the CEN and cell cycle gates have been drawn.

Results & Discussion:

1. Results with the TK6 cell line

We treated our cells with MNNG or temozolomide. We used a dose range of 0 to 480μM for temozolomide and 0 to 1μg/mL for MNNG (figures 10 and 11). Both of these drugs' main cytotoxic lesions are O^6MeG and 3MeA. A frontline repair pathway used by cells to repair the induced damage is direct removal of the methyl adducts with the suicide repair protein O^6-methylguanine-DNA methyltransferase (MGMT). It has previously been reported that cells lacking MGMT are particularly sensitive to such alkylating agents [48]. It is therefore not surprising that the B lymphoblastoid cell line TK6, which also lacks MGMT, is extremely sensitive to both drugs.

2. Dynamic range

With the dose ranges used (ie 0-480μM for temozolomide and 0-1μg/mL for MNNG), the growth inhibition dose-response curves for our twenty-four lymphoblastoid cell lines from twenty-healthy individuals of diverse ancestry span two logs. This is very large, and in the case of temozolomide—where all twenty-four cell lines were assayed—allows us to partition the cell lines into three groups: i) the very resistant cell lines, from most resistant to least resistant: cell lines #7, 3,16 and 14, ii) the mildly sensitive cell lines, # 21, 22, 6, 8, 13, 12, 19, 23, 17, 1, and 20, and iii) the very sensitive cell lines, # 9, 11, 5, and 4. This ranking is based on their sensitivity at the 480 μM. At the 0.5μg/mL dose for MNNG, which is approximately equivalent to the 480 μM dose of temozolomide, the order of the cell lines, from most resistant to most sensitive, is: #16, 14, 23, 21, 6, 20, 17, 11, 5, and 4. This is almost exactly the same order as the one they are in for the temozolomide growth inhibition dose-response curves. From these observations we can conclude that temozolomide and MNNG have very similar cytotoxic powers.

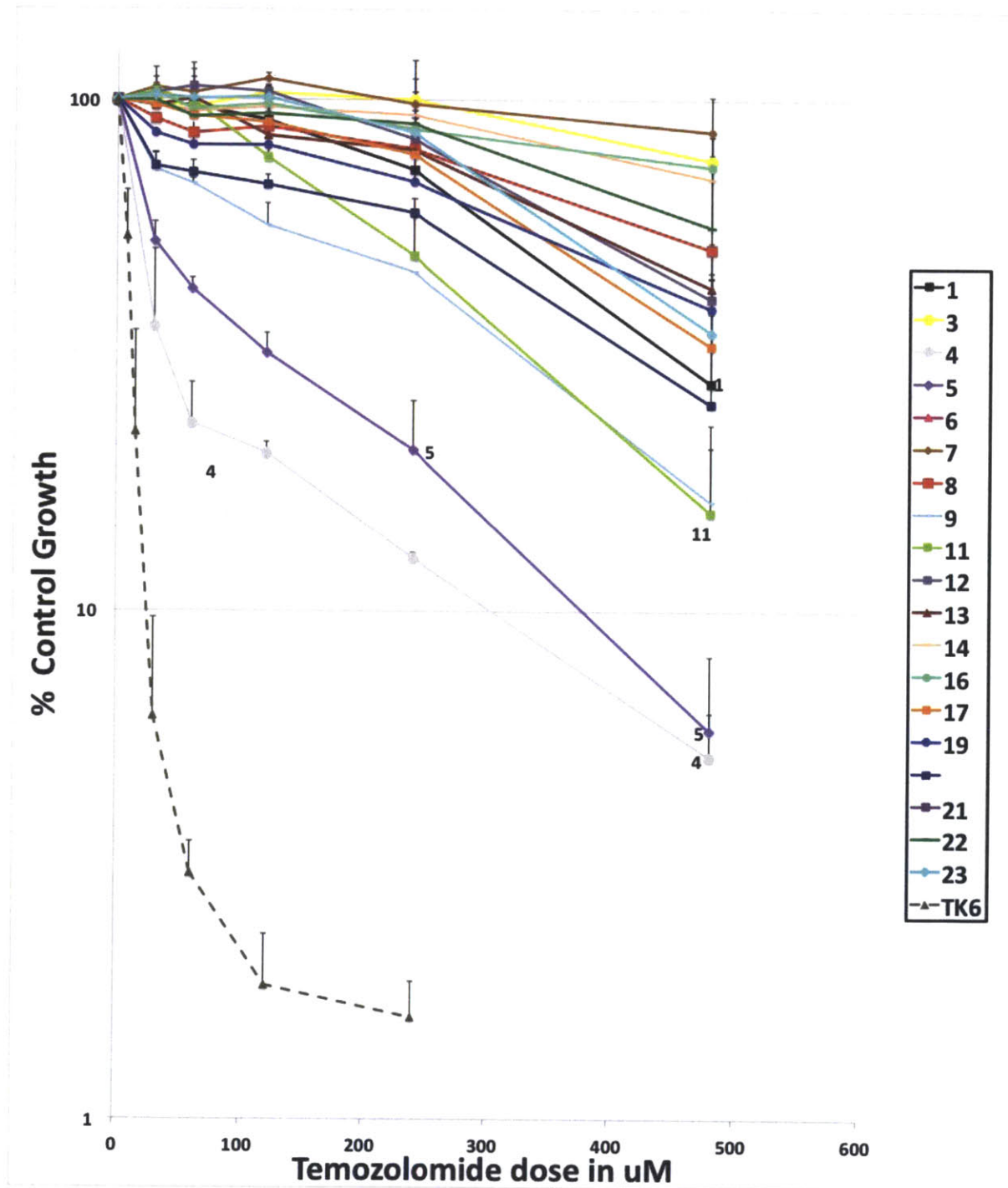**Figure 10: Survival curves for the 24 cell lines after temozolomide treatment**

Survival curves for the panel of 24 genetically varied cell lines for temozolomide doses of 0, 30, 60, 120, 240 and 480μM
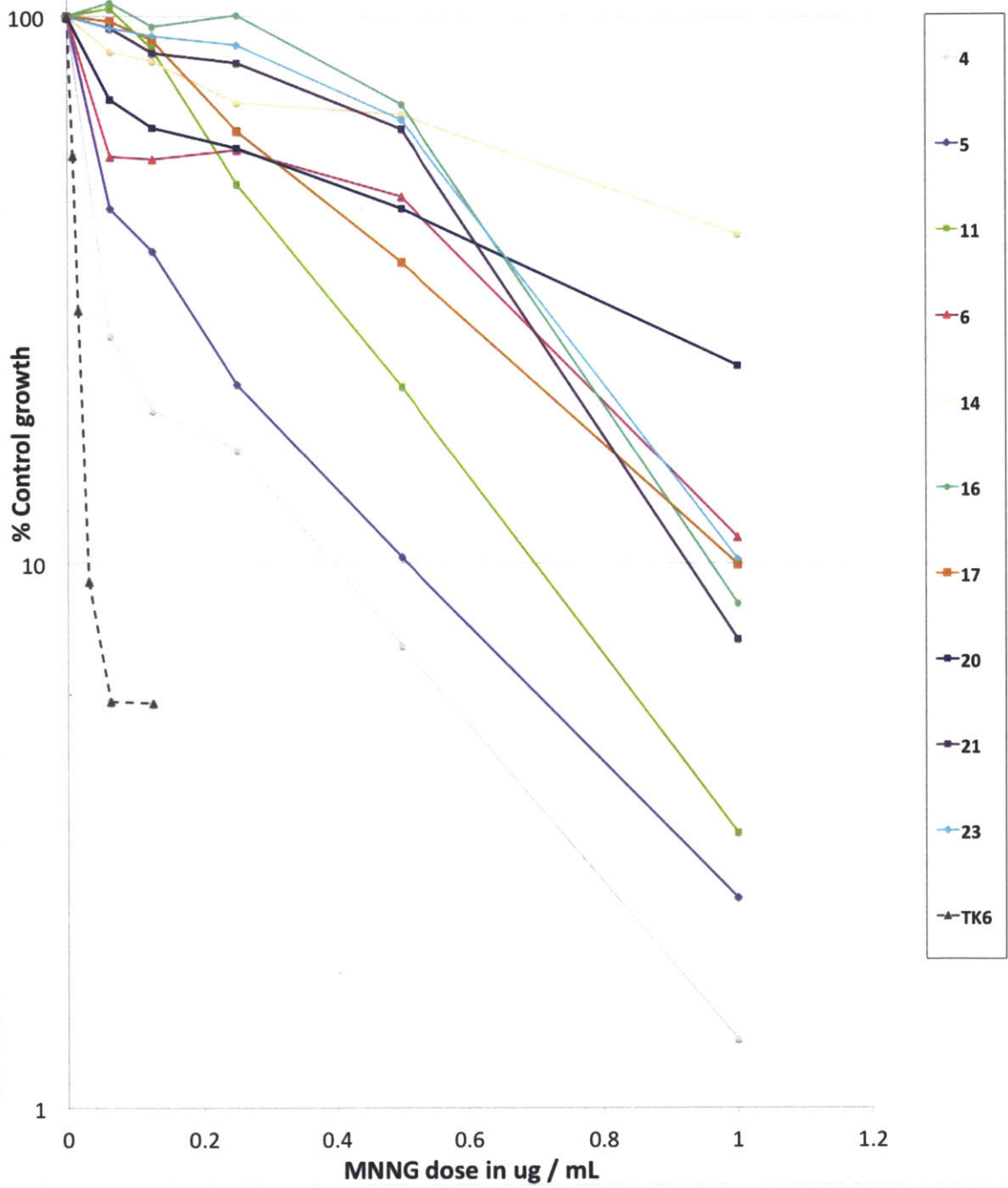
Figure 11: Survival curves for the 24 cell lines after MNNG treatment

Survival curves for the panel of 24 genetically varied cell lines for MNNG doses of 0, 0.0625, 0.125 0.25, 0.5 and 1 μg/ml

3. Dose response profiles for MNNG and temozolomide are different than with BCNU

The advantage of a dose response curve is that is allows us to see the killing profiles of each cell line. This high-throughput growth inhibition assay had already been conducted in the Samson lab using the DNA damaging drug BCNU (figure 12) [5]. The profiles in that case were similar in all the cell lines: linear when plotted on a log scale. For temozolomide and MNNG however, beyond displaying different absolute sensitivities at any given dose, the twenty-four cell lines also display different profiles for their dose response curves (all curves are plotted in log scale). Furthermore, for each cell line tested for MNNG and for temozolomide sensitivity, the profiles are the same with both drugs. For some (e.g. #6 and #1), the slopes are very steep for the lower doses, and then the curves reach a plateau. For others (e.g. #11), the slope is very gentle for the lower doses, and then becomes steeper as the dose increases. Finally, some cell lines (e.g. #5) have a linear dose response. We can conclude that for both drugs, the cells solicit the same DDR mechanisms as the amount of damage increases. These are not the same mechanisms that are solicited in response to BCNU induced damage.

4. The high-throughput assay was able to capture the cell cycle effects of temozolomide or MNNG treatment on the cells:

Our flow cytometry plots show that as the doses of drug (whether it be MNNG or temozolomide) increase, the total number of live cells decreases. The plots also reveal that for all cell lines, increasing doses of drug lead to a rise in the fraction of cells in late S and G2/M phase of the first cell cycle. This fraction corresponds to cells that did not divide during their time in BrdU, and instead stayed arrested in G2/M or late S (figure 13).
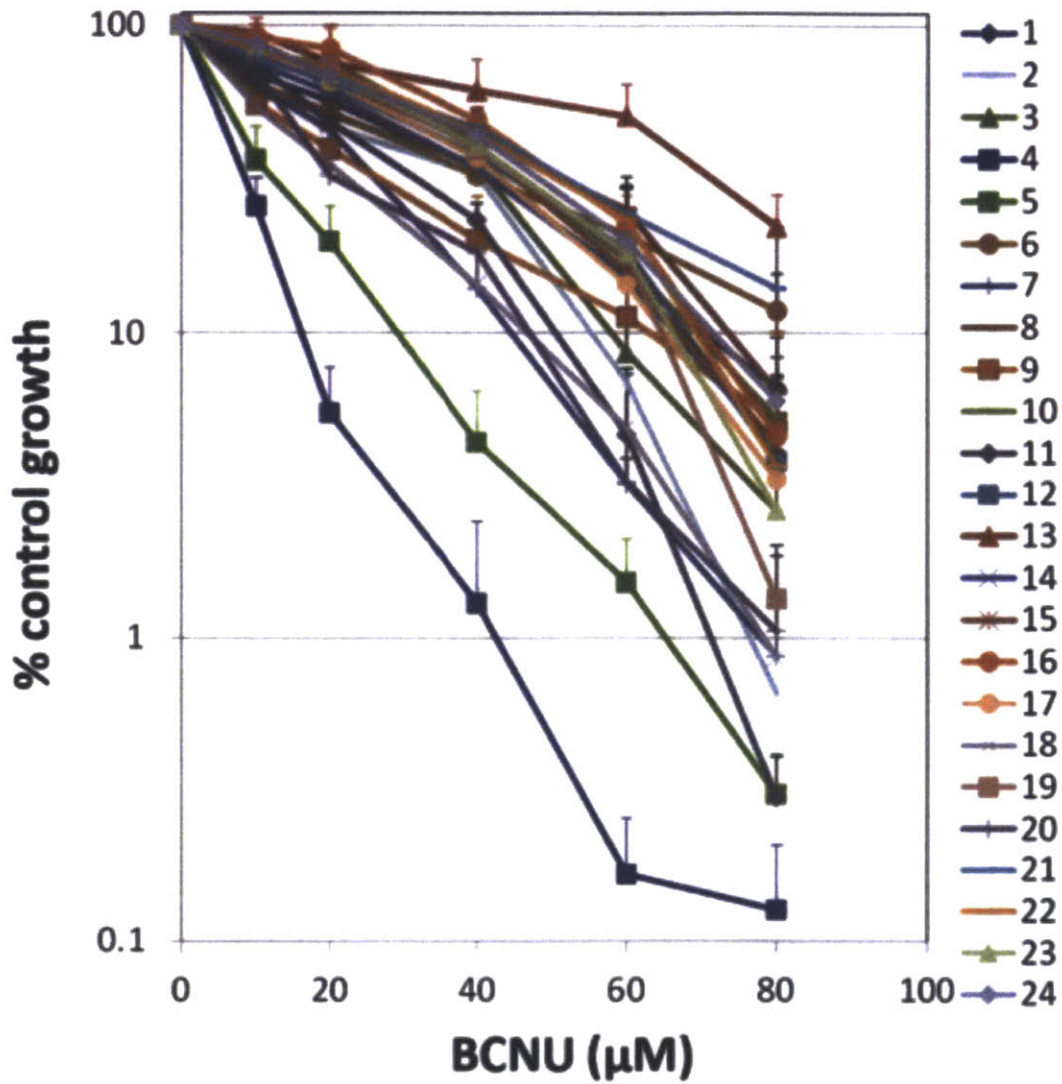
Figure 12: Survival curves for the 24 cell lines after BCNU treatment (by Chandni Valiathan)
Survival curves for the panel of 24 genetically varied cell lines for BCNU doses of 0, 10, 20, 40, 60 and 80 μM. Graphs were obtained by Chandni Valiathan, using the growth inhibition assay described earlier
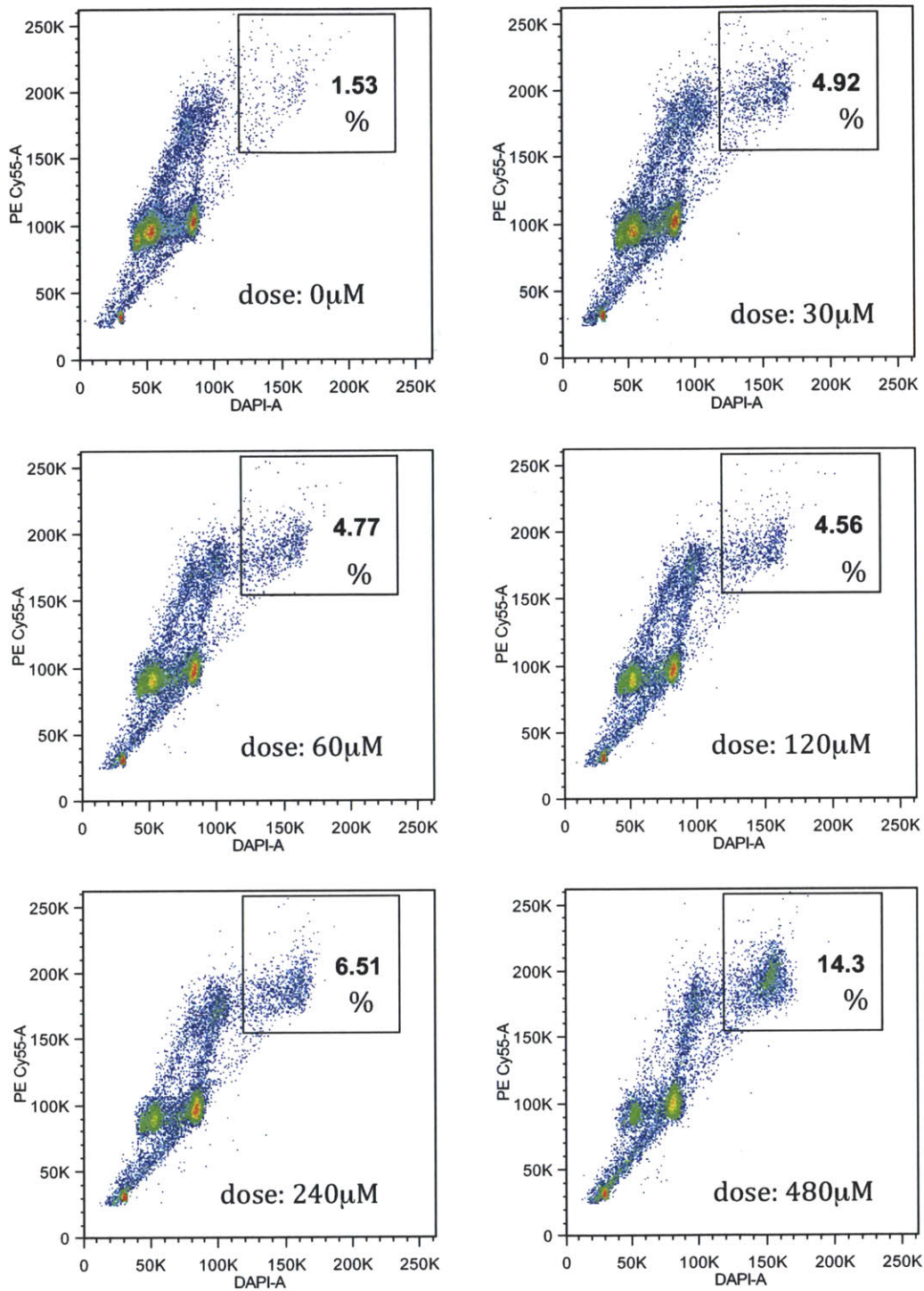
Figure 13: The high-throughput assay was able to capture the cell cycle effects of temozolomide or MNNG treatment on the cells

- Representative example of the gated PI-Area vs. Hoechst-Area data for cell line #5, at doses 0, 30, 60, 120, 240, and 480μM of temozolomide.
- The cells that are in the late G2/M phase of the first cell cycle are boxed. The percentage of all cells that they represent is indicated in the box.

2. Sister chromatid exchange assay

<u>Introduction:</u>

We used a high-throughput FACS based assay to measure the relative amounts of growth inhibition of the Coriell panel of cell lines after treatment with temozolomide. However, growth inhibition is only one of many DNA damage endpoints. Indeed, while this assay gives us a good idea of which cell lines die or arrest most after alkylation damage, it does not tell us how the other damage coping mechanisms are being solicited in each cell line.

One way cells can bypass DNA damage is through homologous recombination[49]. Temozolomide induced damage can lead to a futile repair cycle that is unable to remove the damaged O^6-methylguanine in O^6-methylguanine-Thymine mismatches. This eventually leads to double strand breaks. Furthermore, the close accumulation of DNA nicks and abasic sites due to base excision repair and nucleotide excision repair can also eventually lead to double strand breaks (DSBs) in the DNA. Homologous recombination (HR) is one of the most common ways a cell can repair these DSBs.

We wanted to measure the amounts of homologous recombination in the Coriell set of cell line in order to determine whether or not amounts of HR always correlated with amount of growth inhibition post temozolomide induced damage. One would expect that a sensitive cell line would have very strong growth inhibition post treatment, while having high amounts of homologous recombination. However, a particular cell line could be very sensitive to the damage as far as growth inhibition goes, and have very low amount of HR, indicating that the cell death process is the more solicited response. For the resistant cell lines, some could have low growth inhibition post damage and low amounts of homologous recombination—indicating that the cells repair the damaged bases very efficiently

before they lead to DSBs or signal for cell death. However, other resistant cell lines could have low growth inhibition post damage with high amounts of HR. These cell lines would be strongly soliciting HR in order to avoid cellular death or senescence.

Distinctive homologous recombination (HR) pathways exist, such as synthesis-dependent strand annealing (SDSA) and double-strand break repair (DSBR). After DSB formation, the DNA ends are resected to form 3 single-strand DNA (ssDNA) overhangs. The HR protein machinery then executes strand invasion of a partner chromosome. After a successful homology search, strand invasion occurs to form a D-loop structure. DNA synthesis then ensues. In the SDSA pathway, the D loop is unwound and the freed ssDNA strand anneals with the complementary ssDNA strand that is associated with the other DSB end. The reaction is completed by gap-filling DNA synthesis and ligation. Only noncrossover products are formed. Alternatively, the second DSB end can be captured to form an intermediate that harbors two Holliday junctions (HJs), accompanied by gap-filling DNA synthesis and ligation (figure 14). The resolution of HJs can result in either noncrossover or crossover products [1].

The sister chromatid exchange assay uses the fact that BrdU can incorporate into the DNA of actively replicating cells to measure the amounts of crossover products induced by homologous recombination. The number of these crossover products is considered to be a surrogate marker for the overall amount of homologous recombination[50,51]. In the SCE assay, cells—treated or not with different doses of temozolomide—are left to proliferates with BrdU in their media for the duration of two cell doubling times. As the cells replicate, BrdU is incorporated into the newly synthesized DNA, instead of thymine. Therefore, after a first round of replication, the cells contain DNA that has one strand that contains BrdU and another that does not. The cells then replicate their DNA a second time. Right before dividing again, they have paired sister chromatids in which one chromatid has BrdU incorporated into both strands, and the other has BrdU

incorporated into only one of two strands (figure 15). For our experiments, it is at that moment that we arrested our cells in metaphase, and made metaphase spreads to visualize the sister chromatids.

Hoechst dye preferentially binds AT-rich regions in the DNA, and is quenched by BrdU; we therefore used Hoechst dye to stain our cells' chromosomes. As a result, the sister chromatids were differentially stained, with the sister chromatid that had BrdU incorporated into both strands being lighter[52]. This allowed us to visualize all the crossover events that happened during the second round of DNA replication. Indeed, such crossover events result in "harlequin" stained chromosomes, as shown in figure 16.
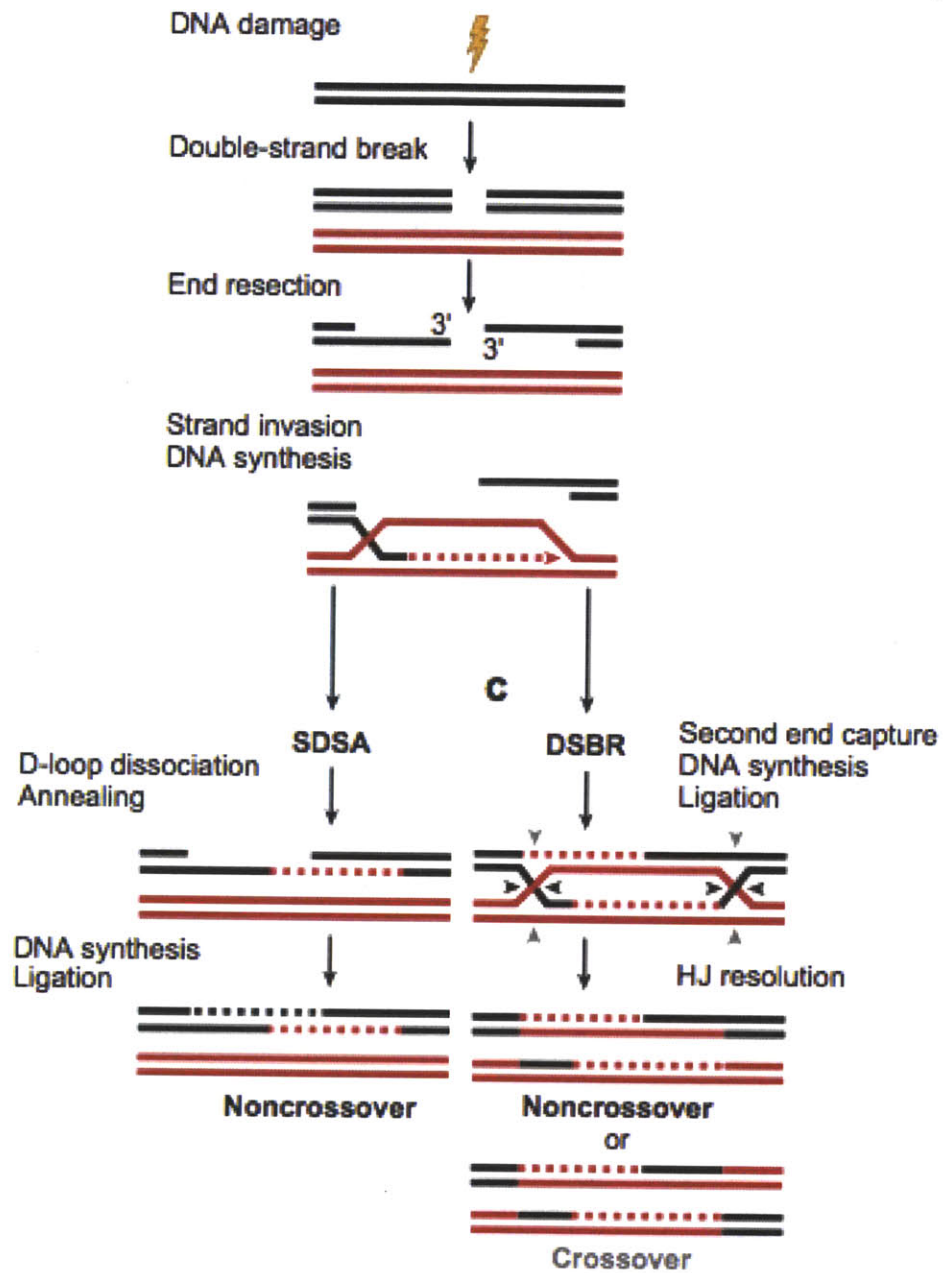
Figure 14: Pathways of DNA double strand break repair by homologous recombination

Adapted from [1]
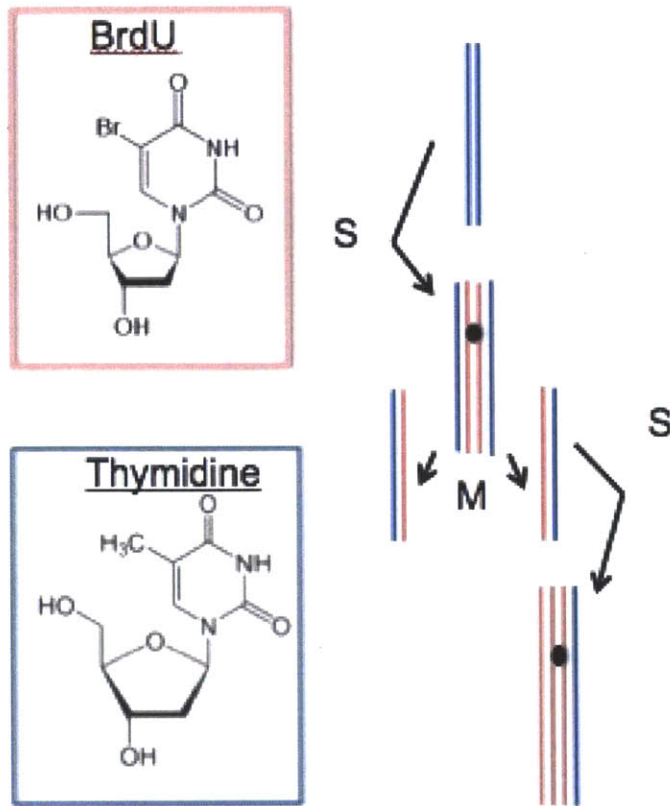
Figure 15: Schematic representation of BrdU incorporation into the DNA of replicating cells

DNA strands that have incorporated BrdU are represented in pink, those that have not are represented in blue.
Chromatids that have incorporated BrdU into both strands are lighter after our staining step than the ones that have incorporated BrdU into only one of two strands.
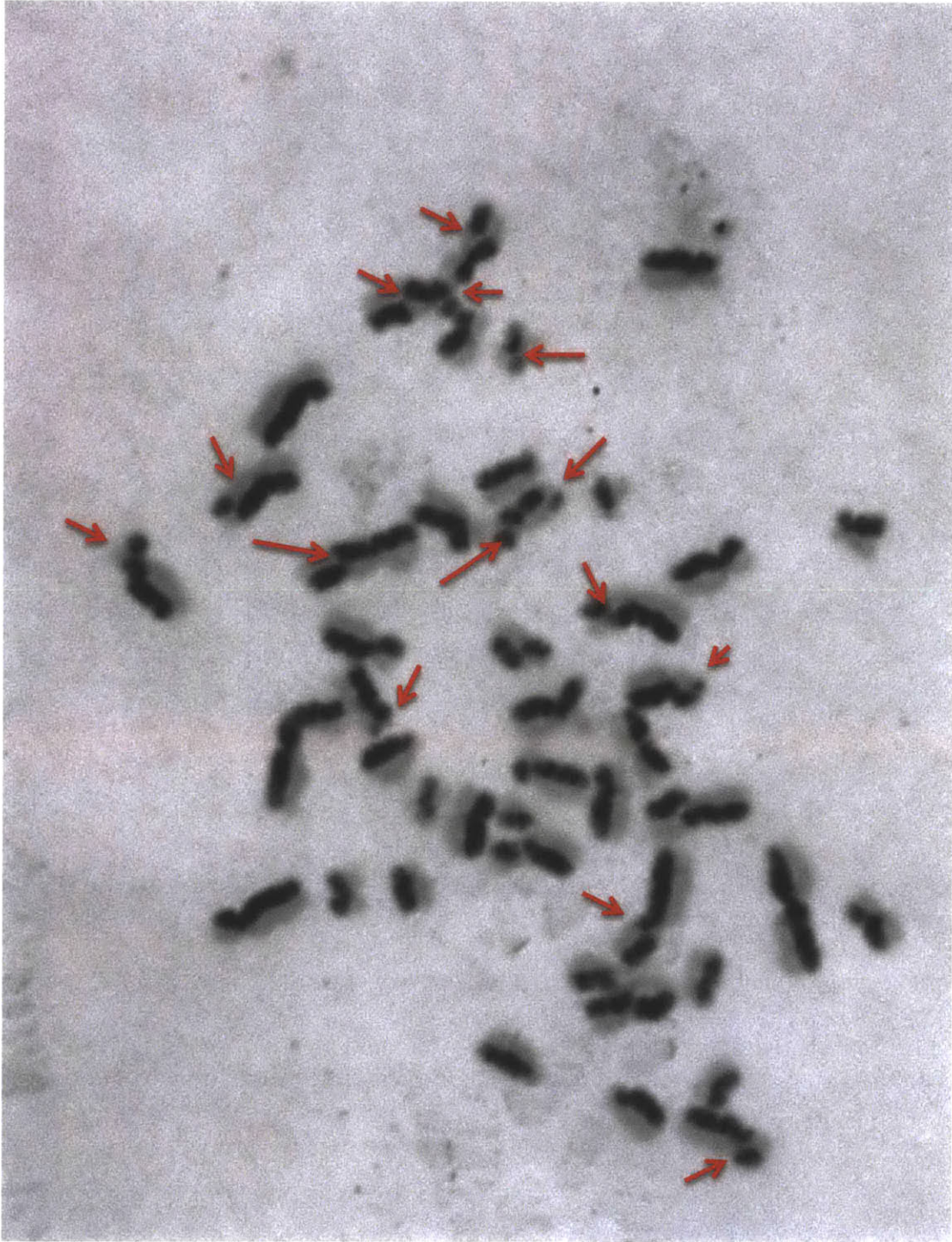
Figure 16: Representative picture of a metaphase spread obtained with our SCE assay

This black and white picture shows one of the metaphase spreads that were found for cell line #8 at a dose of 120μM. The read arrows indicate sites where a sister chromatid exchange occurred.

Results and Discussion:

1. Results with the TK6 and TK6 + MGMT cell lines

We treated our cells with temozolomide. We used a dose range of 0 to 120µM for the Coriell panel of cell lines, and a range of 0 to 30µM for the TK6 cell line (figure 17).

Temozolomide's main cytotoxic lesions are O^6MeG and 3MeA. A frontline repair pathway used by cells to repair the induced damage is direct removal of the methyl adducts with the enzyme O^6-methylguanine-DNA methyltransferase. MGMT. It has previously been reported that cells lacking MGMT are particularly sensitive to such alkylating agents. It is therefore not surprising that the B lymphoblastoid cell line TK6, which lacks MGMT, has very high amounts of temozolomide-induced SCE's. In fact, in was not possible to obtain a sufficient amount of metaphase spreads to reliably measure SCEs for doses higher that 30µM. We also performed the assay on the TK6 + MGMT cell line. This is a TK6 cell line in which MGMT has been reconstituted and is overexpressed. Not surprisingly, the TK6 + MGMT cell line is very resistant to SCE induction through temozolomide treatment. The levels of induced SCE's are baseline for doses up to 120µM.

2. Broad range of sensitivity for the Coriell panel of cell lines

The Coriell panel of cell lines displayed a broad range of sensitivity to temozolomide for the growth inhibition assay. Similarly, the cell lines display a broad range of sensitivity for the SCE assay. The TK6 cell line had the highest induction of SCEs. For the Coriell cell lines, the number of SCEs at the 120µM dose of temozolomide ranged from 0.006 SCE's per chromosome (cell line #22) to 0.65 SCE's per chromosome (cell line #4). This represents a 100 fold range.

3. Number of induced SCEs generally correlates with the cell lines' growth inhibition profiles

Most of the cell lines' growth inhibition dose response profiles correlated strongly to their SCE induction results. Cell lines #4 and #5 were the two most sensitive cell lines in the growth inhibition assay, with #4 being more sensitive than #5. This was also observed for the SCE endpoint: #4, then #5, are the two cell lines with the highest amounts of induced SCE's per chromosome at any dose. Furthermore, cell lines #22 and #8 were among the most resistant in the growth inhibition assay, and they were also among the most resistant in the SCE assay. In general, most of the cell lines' sensitivities for the growth inhibition endpoint correlated with their sensitivities for the SCE endpoint.

From these observations we can infer that, for the cell lines tested, sensitivity to temozolomide, as far as growth inhibition in concerned, correlates to high amounts of induced SCE's, while resistance correlates with low amounts of induced SCE's.
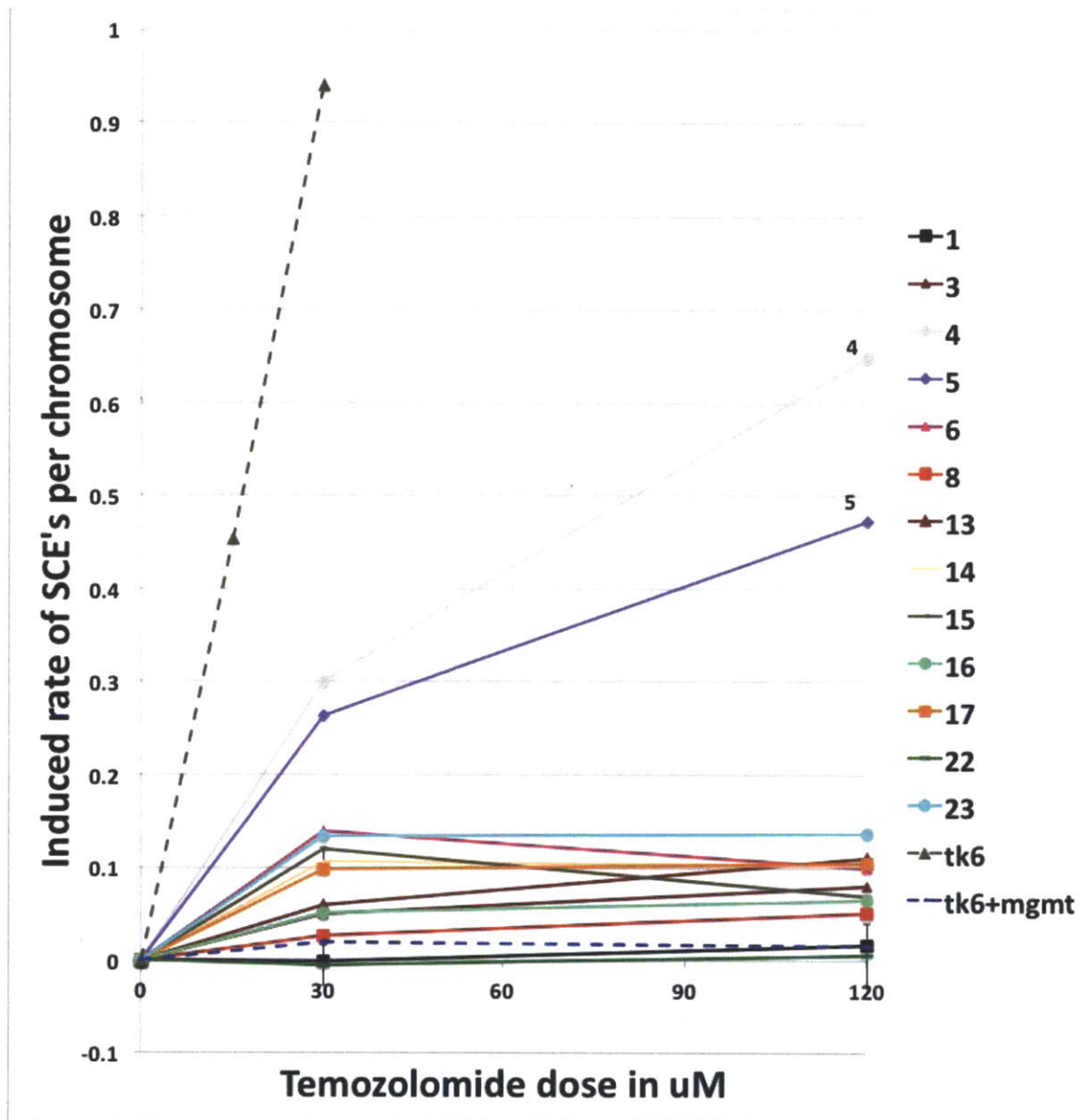
Figure 17: Induced sister chromatid exchange rates for the 24 cell lines after temozolomide treatment

SCE curves for the panel of 24 genetically varied cell lines for temozolomide doses of 0, 30, and 120μM

Materials and Methods:

1. Tissue Culture

The 24 lymphoblastoid cell lines, established using EBV transformation, were obtained from the Coriell Institute and were designated 1–24 as follows: #1 (GM15029), #2 (GM15036), #3 (GM15215), #4 (GM15223), #5 (GM15245), #6 (15,224), #7 (GM15236), #8 (GM15510), #9 (GM15213), #10 (GM15221), #11 (GM15227), #12 (GM15385), #13 (GM15590), #14 (GM15038), #15 (GM15056), #16 (GM15072), #17 (GM15144), #18 (GM15216), #19 (GM15226), #20 (GM15242), #21 (GM15268), #22 (GM15324), #23 (GM15386), and #24 (GM15061).

These cell lines, as well as the lymphoblastoid cell line TK6, were grown in suspension in RPMI medium supplemented with 15% fetal bovine serum, 1% glutamine, and 1 % penicillin-streptomycin. All assay were set up using logarithmically growing cells.

The 24 cell lines were ordered based on their normal doubling time, then partitioned into four groups, as detailed in table 1 Cell lines in each group were assayed based on the approximate doubling time for the group.

Cell line	Doubling time (hours)	Approximated doubling time (hours)
8	17	18
22	19	
21	20	22
20	20	
16	21	
24	21	
6	22	
14	22	
1	22	
17	22	
3	23	
5	24	
15	24	
23	24	
12	25	27
13	25	
9	26	
19	27	
7	27	
2	28	
4	30	
11	30	
18	35	37
10	40	

Table 1: Doubling times for all 24 cell lines, and approximated doubling times

The cell lines were divided into four groups of lines with similar doubling times. The assays were conducted using their approximated doubling times. This allowed us to handle several cell lines at a time.

2. Flow cytometry based growth inhibition assay

<u>Temozolomide treatment:</u>

Cells were grown to mid-log phase. Cells were spun and resuspended in serum-free media. 270 µl of cells at a density of 4.5x10 5 cells/ml were plated in each well of one row of a V-bottom 96-well plate. If multiple cell lines were assayed, each cell line was plated in one row of a 96-well plate.

The drug was diluted to lOX of the final dose concentrations in serum-free media in another 96-well plate. 30µl of the lOX drug was transferred to each well in the 96-well plate containing cells, after which the cells were incubated at 37°C for lh. After lh, cells were spun down at 1500rpm for 5min. Drug-containing media was removed and the cells were washed with 200µl warm 1XPBS per well. The cells were then resuspended in 280uL of warm media containing serum, transferred to a flat-bottom 96-well plate and incubated at 37°C for the duration of two doubling times.

<u>MNNG treatment:</u>

Cells were grown to mid-log phase. 270 µl of cells at a density of 2.5x10 5 cells/ml were plated in each well of one row of a flat-bottom 96-well plate. If multiple cell lines were assayed, each cell line was plated in one row of a 96-well plate.

The drug was diluted to lOOX of the final dose concentrations in serum-free media in another 96-well plate. 3µl of the lOOX drug was transferred to each well in the 96-well plate containing cells. The cells were then incubated at 37°C for the duration of two doubling times.

BrdU addtion

After allowing cells to respond for two doubling times after drug treatment, the cells are incubated in the presence of BrdU for another two doubling times. The optimal BrdU concentration was determined to be 45pM for the Coriell cell lines as well as for TK6.

A the first two doubling times, BrdU was added to the treated cells at a concentration of 45μM (from a 10mM stock). BrdU was replenished every 12 hours after this start, by adding an extra 45μm to each well. This was done for the duration of two more cell cycles.

Sample preparation for FACS

At the end of four doubling times after drug treatment, cells were transferred to a V-bottom 96- well plate using a multi-channel pipette. The plate was spun down at 1500rpm for 5min. The media was removed and cells were washed with 200μL of cold 1XPBS.

The cells were then resuspended in 280uL of lX lysis buffer (0.1M Tris HCI pH 7.5, 0.1% Igepal CA-60, 1mM CaCl2, 5mM MgC12, 0.2%BSA (w/v), 1.2μg/ml Hoechst 33258 and lx104 chicken erythrocyte nuclei (CEN)/ml) and incubated on ice *for 15* minutes. Two wells containing only the lysis/staining buffer and propidium iodide are also prepared as blanks

Before running each sample, it was transferred to a flow cytometry tube, and 12μl of 100μg/ml propidium iodide was added. Each sample was then briefly vortexed, and analyzed on a BD LSR II flow cytometer.

Data Collection

Events were visualized on the side scatter vs. forward scatter plot to gate out debris, and on the PI-height vs. PI-area plot to exclude doublets that fall below the diagonal. The voltages for PI and Hoechst were adjusted to position the chicken erythrocyte nuclei at the (30K, 30K) point to facilitate subsequent data analysis. 15 000 events that passed the two selection criteria were collected and viewed on a PI- Area vs. Hoechst-Area plot.

Data Analysis

All data were analyzed using FlowJo software (TreeStar Inc). For each cell line and drug dose, the debris and doublets were gated out. The remaining events were observed on a PI-Area vs. Hoechst-Area plot. The regions corresponding to cells in the 1st, 2nd or 3rd cell cycle post BrdU addition were gated. Hoechst fluorescence of cells decreases as they incorporate BrdU during DNA replication. Therefore, as the cells replicate and divide, they move from the region labeled 1st cell cycle to the region labeled 2nd cell cycle, to the region labeled 3rd cell cycle. For each sample, the number of events in each gate was determined. The CEN were also gated (around 30k, 30k) in order to normalize the number of cells in each sample.

The normalized fraction of proliferating cells post treatment is given by the formula:

1/2 * (# of events in cell cycle 2) / # CEN + 1/3 * (# of events in cell cycle 3) / # CEN

The ratio of proliferated cells in a treated sample to that in an untreated sample gives the **%** control growth value that is used to plot a survival curve.

3. Sister Chromatid Exchange assay

Temozolomide treatment

Cells were grown to mid-log phase. Cells were spun and resuspended in 50mL Falcon tubes in 18mLs of serum-free media at a concentration of $5*10^5$ cells/mL. Each dose corresponded to one tube. The drug was diluted to 10X the final dose concentrations. 2mLs of 10X drug was added to the corresponding dose tube.

After 1h, cells were spun down at 1500rpm for 5min. Drug-containing media was removed and the cells were washed with 10mLs of warm 1XPBS. The cells were then resuspended in 15mLs of serum containing media supplemented with 10μM of bromodeoxyuridine (BrdU, 1:100 dilution of 1mM stock). The cells were transferred to a 25cm3 cell culture flask and returned to the incubator for the duration of 2 normal doubling times.

Obtaining metaphase spreads

After complete BrdU incubation, 0.1μg/ml of Colcemid (1:1000 dilution of a 0.1mg/ml stock solution) was added to each flask and then left to incubate for 2 more hours. The contents of each flask were then transferred to a 15mL Falcon tube. The cells were then spun at 100g for 5min. The supernatant was aspirated, leaving a small volume of liquid remaining, in which the cells were then resuspended. 5mLs of hypotonic solution were then added very slowly to each tube, drop by drop, in order to avoid that the cells burst prematurely. The cells were then incubated in hypotonic solution at 37C for 15min.

Following hypotonic treatment, the tubes were centrifuges for 5min. The majority of the supernatant was aspirated, and the cell pellet resuspended in the remaining volume as done previously. The cells were then slowly resuspended in 5

mLs of Carnoy's fixative (3 MeOH:1 Acetic Acid). The samples were again spun for 5min at 100g, the supernatant almost entirely aspirated and the cells resuspended in the remaining liquid volume, and the cells slowly resuspended in 5mLs of Carnoy's fixative. The cells were the spun 5min again, and the supernatant aspirated leaving approximately 1mL of liquid in the tube to resuspend the cells in.

The cells were then dropped onto microscope slides, from a height of 12-18 inches, using a Pasteur pipette. 4-5 drops were placed on each slide. The slides were left to dry overnight.

Harlequin staining of chromosomes

Slides were placed in coplin jars and stained for 20min in a 5μg/ml Hoechst solution (a 50μg/ml Hoechst stock solution was diluted 1:10 in 1x Sorensen's phosphate buffer, itself made for a 10X stock containing: 0.335M of Na_2HPO_4 and 0.335M of KH_2PO_4). The slides were then rinsed with water, blotted to remove excess fluid, and left to air dry.

A few drops of 1X Sorensen's buffer was then dropped onto each slide, and the slides were mounted with a rectangular coverslip. These slides were placed onto a 65°C slide warmer and exposed to black light for 20min.

After 20min under black light, the slides were taken off of the slide warmer. The coverslips were removed, the slides rinsed with water, blotted to remove excess water, and again left to air dry. A large drop of 20X SSC buffer (3M of NaCl and 300mM of sodium citrate in water) was placed onto each slide, the slides mounted with a rectangular coverslip, and placed back onto a 65°C slide warmer for an additional 20min.

The slides were then taken off of the slide warmer, and rinsed after their coverslips were removed. The excess water was blotted and the slides were left to air dry. The slides were incubated for 8min in 5% Giemsa staining solution (1:20 dilution in Sorensen's buffer), then rinsed with water, and left to dry fully. The slides were dipped in histological grade xylene, then two or three drops of Permount mounting solution was placed on each slide, and they were mounted with a rectangular coverslip and left to dry completely.

Microscopy and image analysis

Spreads were scanned with bright field microscopy at a low power (10, 20x) to first find second division cells. During replication the cells incorporated the BrdU into their newly synthesized DNA. Therefore at the metaphase of the first cellular division, sister chromatids both contain one strand that has incorporated BrdU (figure 15). At the metaphase of the second cell division, one sister chromatid has only one strand that has incorporated BrdU, while the second has incorporated it into both strands (figure 15). In second division cells the Hoechst fluorescence of two sister chromatids will therefore be different. After Giemsa staining this translates into one chromatid stained dark purple or pink, with the sister chromatid stained a lighter pink (figure 16).

20 second division metaphase spreads were then photographed at a power of 100x. For each spread the number of chromosomes, and the number of exchanges were counted using ImajeJ software. Then the average number of exchanges per chromosome across all 20 spreads was calculated.

Conclusions and Future Directions

A few key results were shown in this thesis. We have first and foremost shown—through the use of a high-throughput highly sensitive growth inhibition assay with a broad range of sensitivity—that while our Coriell panel of cell lines display a very broad range of sensitivity to MNNG and temozolomide, their relative sensitivities to both drugs are very similar. Several conclusions can be drawn from this observation. First of all, the implicit assumption that temozolomide and MNNG are so similar in their mode of toxicity that they can be used and referred to interchangeably is not in contradiction with this study. Since MNNG has for a long time been a key model alkylating agent for toxicity studies, while temozolomide is being used in the clinic today, this apparent interchangeability is of great scientific relevance. Second of all, since these cell lines were derived from different healthy individuals, we can infer that this similarity in sensitivity ranking would also be observed in these individuals. We can thus conclude that an approximation of an individual's sensitivity to MNNG can be determined by examining in a large population his or her relative sensitivity to temozolomide, as well as the sensitivities of that population to MNNG (and vice-versa).

In most of the cell lines we tested, there was a positive correlation between the sensitivity to growth inhibition and the sensitivity to SCE induction. This is consistent with the idea that if a cell line is sensitive, it is more likely to accumulate damage that processes such as homologous recombination will mediate. We did however find one cell line that was quite sensitive to temozolomide as far as growth inhibition goes, all the while having very low amounts of induced SCEs. We can conclude that this cell line resorts to cell death and cell cycle arrest but not as much to homologous recombination.

Some supplementary studies would be needed to strengthen our conclusions. Testing larger numbers of individuals, or cell lines derived from individuals, would

provide more statistical confidence that a given individual's sensitivities to temozolomide and MNNG are similar. As for the SCE's induced by temozolomide, while for the sensitive cell lines it is difficult to obtain second division metaphase spreads for doses higher than 120μM, it would be of interest to examine the induced SCEs for doses larger than 120μM in the resistant cell lines. Indeed this would allow us to further distinguish and rank the SCE resistant individuals among themselves.

While these DNA damage phenotypes reveal important information in themselves, it is their correlation to systems-wide data that would make it possible to predict the sensitivity of yet unstudied cell lines to temozolomide and MNNG. Furthermore, a systems-wide study would also allow us to gain insight into what makes some cell lines sensitive for one DNA damage endpoint (e.g. growth inhibition) and not another (e.g. homologous recombination). This systems-wide data could be proteomic, transcriptomic (mRNAs, miRNAs, etc...), genetic, or epigenetic. Since DNA damage solicits a very broad response that involves multiple processes in the cell, one could imagine that several genome wide datasets of different types, taken separately, could have predictive value. Finally, integrating these genome-wide datasets could provide even more predictive strength.

References

1. San Filippo, J., Sung, P. & Klein, H. Mechanism of eukaryotic homologous recombination. *Annu Rev Biochem* **77**, 229-257 (2008).
2. Hegi, M.E., *et al.* Correlation of O6-methylguanine methyltransferase (MGMT) promoter methylation with clinical outcomes in glioblastoma and clinical strategies to modulate MGMT activity. *J Clin Oncol* **26**, 4189-4199 (2008).
3. Fry, R.C., *et al.* Genomic predictors of interindividual differences in response to DNA damaging agents. *Genes Dev* **22**, 2621-2626 (2008).
4. Friedman, H.S., Kerby, T. & Calvert, H. Temozolomide and treatment of malignant glioma. *Clin Cancer Res* **6**, 2585-2597 (2000).
5. Valiathan, C., McFaline, J.L. & Samson, L.D. A rapid survival assay to measure drug-induced cytotoxicity and cell cycle effects. *DNA repair* (2011).
6. Hoeijmakers, J.H. DNA damage, aging, and cancer. *N Engl J Med* **361**, 1475-1485 (2009).
7. De Bont, R. & van Larebeke, N. Endogenous DNA damage in humans: a review of quantitative data. *Mutagenesis* **19**, 169-185 (2004).
8. David, S.S., O'Shea, V.L. & Kundu, S. Base-excision repair of oxidative DNA damage. *Nature* **447**, 941-950 (2007).
9. Lindahl, T. Instability and decay of the primary structure of DNA. *Nature* **362**, 709-715 (1993).
10. Bartek, J., Bartkova, J. & Lukas, J. DNA damage signalling guards against activated oncogenes and tumour progression. *Oncogene* **26**, 7773-7779 (2007).
11. Lavin, M.F. Ataxia-telangiectasia: from a rare disorder to a paradigm for cell signalling and cancer. *Nat Rev Mol Cell Biol* **9**, 759-769 (2008).
12. Zhou, B.B. & Elledge, S.J. The DNA damage response: putting checkpoints in perspective. *Nature* **408**, 433-439 (2000).
13. Gaudet, S., *et al.* A compendium of signals and responses triggered by prodeath and prosurvival cytokines. *Mol Cell Proteomics* **4**, 1569-1590 (2005).
14. Calzone, L., *et al.* Mathematical modelling of cell-fate decision in response to death receptor engagement. *PLoS Comput Biol* **6**, e1000702 (2010).
15. Hakem, R. DNA-damage repair; the good, the bad, and the ugly. *The EMBO journal* **27**, 589-605 (2008).
16. Mishina, Y., Duguid, E.M. & He, C. Direct reversal of DNA alkylation damage. *Chemical reviews* **106**, 215-232 (2006).
17. Wilson, D.M., 3rd & Bohr, V.A. The mechanics of base excision repair, and its relationship to aging and disease. *DNA Repair (Amst)* **6**, 544-559 (2007).
18. Gillet, L.C. & Scharer, O.D. Molecular mechanisms of mammalian global genome nucleotide excision repair. *Chem Rev* **106**, 253-276 (2006).
19. O'Driscoll, M. & Jeggo, P.A. The role of double-strand break repair - insights from human genetics. *Nat Rev Genet* **7**, 45-54 (2006).

20. Burma, S., Chen, B.P. & Chen, D.J. Role of non-homologous end joining (NHEJ) in maintaining genomic integrity. *DNA repair* **5**, 1042-1048 (2006).

21. Kai, M. & Wang, T.S. Checkpoint activation regulates mutagenic translesion synthesis. *Genes & development* **17**, 64-76 (2003).

22. Jackson, S.P. & Bartek, J. The DNA-damage response in human biology and disease. *Nature* **461**, 1071-1078 (2009).

23. Workman, C.T., *et al.* A systems approach to mapping DNA damage response pathways. *Science* **312**, 1054-1059 (2006).

24. Hanahan, D. & Weinberg, R.A. Hallmarks of cancer: the next generation. *Cell* **144**, 646-674 (2011).

25. Andressoo, J.O. & Hoeijmakers, J.H. Transcription-coupled repair and premature ageing. *Mutation research* **577**, 179-194 (2005).

26. Vousden, K.H. & Lu, X. Live or let die: the cell's response to p53. *Nat Rev Cancer* **2**, 594-604 (2002).

27. Pennisi, E. Breakthrough of the year. Human genetic variation. *Science* **318**, 1842-1843 (2007).

28. Frazer, K.A., Murray, S.S., Schork, N.J. & Topol, E.J. Human genetic variation and its contribution to complex traits. *Nat Rev Genet* **10**, 241-251 (2009).

29. Hamburg, M.A. & Collins, F.S. The path to personalized medicine. *The New England journal of medicine* **363**, 301-304 (2010).

30. Weinstein, J.N. Pharmacogenomics--teaching old drugs new tricks. *The New England journal of medicine* **343**, 1408-1409 (2000).

31. van't Veer, L.J. & Bernards, R. Enabling personalized cancer medicine through analysis of gene-expression patterns. *Nature* **452**, 564-570 (2008).

32. Roses, A.D. Pharmacogenetics and the practice of medicine. *Nature* **405**, 857-865 (2000).

33. Meyer, U.A. Pharmacogenetics and adverse drug reactions. *Lancet* **356**, 1667-1671 (2000).

34. Pauling, L., Itano, H.A. & et al. Sickle cell anemia, a molecular disease. *Science* **109**, 443 (1949).

35. Evans, W.E. & McLeod, H.L. Pharmacogenomics--drug disposition, drug targets, and side effects. *The New England journal of medicine* **348**, 538-549 (2003).

36. Stupp, R., *et al.* Radiotherapy plus concomitant and adjuvant temozolomide for glioblastoma. *The New England journal of medicine* **352**, 987-996 (2005).

37. Denny, B.J., Wheelhouse, R.T., Stevens, M.F., Tsang, L.L. & Slack, J.A. NMR and molecular modeling investigation of the mechanism of activation of the antitumor drug temozolomide and its interaction with DNA. *Biochemistry* **33**, 9045-9051 (1994).

38. Hegi, M.E., *et al.* MGMT gene silencing and benefit from temozolomide in glioblastoma. *The New England journal of medicine* **352**, 997-1003 (2005).

39. D'Atri, S., *et al.* Involvement of the mismatch repair system in temozolomide-induced apoptosis. *Mol Pharmacol* **54**, 334-341 (1998).

40. O'Brien, V. & Brown, R. Signalling cell cycle arrest and cell death through the MMR System. *Carcinogenesis* **27**, 682-692 (2006).

41. Wyatt, M.D. & Pittman, D.L. Methylating agents and DNA repair responses: Methylated bases and sources of strand breaks. *Chem Res Toxicol* **19**, 1580-1594 (2006).

42. Sugimura, T., Nagao, M. & Okada, Y. Carcinogenic action of N-methyl-N'-nitro-N-nitrosoguanidine. *Nature* **210**, 962-963 (1966).

43. Hargrave, D.R., *et al.* Phase I study of fotemustine in pediatric patients with refractory brain tumors. *Cancer* **95**, 1294-1301 (2002).

44. Briegert, M. & Kaina, B. Human monocytes, but not dendritic cells derived from them, are defective in base excision repair and hypersensitive to methylating agents. *Cancer Res* **67**, 26-31 (2007).

45. McEllin, B., *et al.* PTEN loss compromises homologous recombination repair in astrocytes: implications for glioblastoma therapy with temozolomide or poly(ADP-ribose) polymerase inhibitors. *Cancer Res* **70**, 5457-5464 (2010).

46. Collins, F.S., Brooks, L.D. & Chakravarti, A. A DNA polymorphism discovery resource for research on human genetic variation. *Genome Res* **8**, 1229-1231 (1998).

47. Forte, E. & Luftig, M.A. MDM2-dependent inhibition of p53 is required for Epstein-Barr virus B-cell growth transformation and infected-cell survival. *J Virol* **83**, 2491-2499 (2009).

48. Liu, L. & Gerson, S.L. Targeted modulation of MGMT: clinical implications. *Clin Cancer Res* **12**, 328-331 (2006).

49. Trivedi, R.N., Almeida, K.H., Fornsaglio, J.L., Schamus, S. & Sobol, R.W. The role of base excision repair in the sensitivity and resistance to temozolomide-mediated cell death. *Cancer Res* **65**, 6394-6400 (2005).

50. Johnson, R.D. & Jasin, M. Sister chromatid gene conversion is a prominent double-strand break repair pathway in mammalian cells. *The EMBO journal* **19**, 3398-3407 (2000).

51. Sonoda, E., *et al.* Sister chromatid exchanges are mediated by homologous recombination in vertebrate cells. *Molecular and cellular biology* **19**, 5166-5169 (1999).

52. Korenberg, J.R. & Freedlender, E.F. Giemsa technique for the detection of sister chromatid exchanges. *Chromosoma* **48**, 355-360 (1974).